

Research Article

Unified Navigational Approach for an Autonomous Vehicle Joining a Multilane Highway from Ramp

Usman Ghumman ¹, Kunwar Faraz,¹ Hamid Jabbar,¹ and Mohsin I. Tiwana^{1,2}

¹Department of Mechatronics Engineering, NUST College of E&ME, Rawalpindi 46000, Pakistan

²Robot Design and Development Lab (RDDDL), National Centre of Robotics and Automation (NCRA), NUST College of E&ME, Rawalpindi 46000, Pakistan

Correspondence should be addressed to Usman Ghumman; usman.ghumman@ceme.nust.edu.pk

Received 22 September 2022; Revised 20 October 2022; Accepted 25 October 2022; Published 10 November 2022

Academic Editor: L. Fortuna

Copyright © 2022 Usman Ghumman et al. This is an open access article distributed under the Creative Commons Attribution License, which permits unrestricted use, distribution, and reproduction in any medium, provided the original work is properly cited.

Navigating an autonomous vehicle through a circular ramp to join a multilane highway having high-density traffic is a very challenging task. Occupant and vehicle safety are the major considerations while establishing merging scenarios. This article proposes and experimentally implements safe and tactical navigational procedures for merging and leaving the highway scenario using the rendezvous guidance (RG) technique and its modified form. Test scenarios have been established for navigating AVs to merge and leave the highway on a multilane highway with or without the presence of any other vehicle in the zone. In addition, the navigation with enhanced performance of the modified RG algorithm is also established and compared to the conventional RG algorithm. The results indicate that time is reduced considerably by using the modified RG technique. The experimental and simulation results are compared, and their results are the same.

1. Introduction

Autonomous vehicles (AVs) control is one of the significant artificial intelligence-based applications in the transportation industry. It artificially mimics human driving skills and establishes tactical autonomous drive control. Therefore, AV becomes an important component of an intelligent transportation system (ITS). ITS consists of an advanced driver assistance system (ADAS), which controls and adjusts speed to ensure a safe distance using adaptive cruise control (ACC). Merging into a highway or leaving it is a component of ITS. It can either be used as a driver assistance tool or as a complete autonomous operation. The operation of merging and leaving the highway consists of three basic steps that are adjusting speed, starting the merge, and leaving the driving lane. The operation becomes very difficult during high traffic densities. It has been quoted that 4–10% of collisions are recorded due to wrong tactical decisions [1]. Human comfort, driver and vehicle safety, and collision-free driving in the presence of obstacles, with continuously varying

speeds, can only be ensured when the algorithm is fully aware of parameters that affect decision-making [2]. The concept of AVs is still new in the urban environments in developing countries such as Pakistan, India, and others. However, the adoption rate is increasing day-by-day. 1 out of 9 vehicles is an AV in developing countries, and in the least developed countries, the ratio is even less than 1 out of 15 [3]. Therefore, it is necessary to investigate different factors for the safe operation of AVs. Joining or leaving a highway or convey are the complex operations of AVs, hence require careful handling.

This research work presents the solution to the joining and leaving scenario of a vehicle joining the multilane highway from the sideways through a circular ramp. Two scenarios are presented (merging onto a highway and leaving a highway). In both cases, further permutation includes the presence or absence of any other vehicle in the work space. This research work experimentally implements the above-mentioned scenarios as proofs of concept for RG and its modified form.

This article consists of six sections. First, section covers the introduction. Second, section of the article consists of a literature review with an identification of the research gap. Third, portion explains the problem formulation and mathematical modelling of the proposed technique. Fourth, section covers simulation results and comparative analysis between conventional and modified RG techniques. The experimental setups along with results are discussed in Section 5. Finally, the manuscript is concluded in the last section.

2. Literature Review

Joining or leaving a highway from a ramp by an autonomous vehicle is a part of the middle level decision-making loop, which guides the autonomous vehicle in routine operations. The middle level operations include accident avoidance, overtaking, joining or leaving a highway from a ramp, adjusting speed according to road conditions/environment, and many more. The middle level or one may call it tactical level, decision-making process for autonomous vehicles (AVs) is still the topic in development. The adoption of AVs as a transportation source gives numerous benefits to the society, such as less accidents, driver and vehicle safety, efficient flow of traffic, better fuel economy, and less manoeuvring time [4–7]. Manoeuvring efficiency is one of the key factors in adopting AVs as a source of transportation on modern day roads. Different types and scenarios of manoeuvring are discussed in literature. 4–10% of collisions have been recorded annually among vehicles on the road due to wrong tactical level operations, including joining or leaving the highway operation [8, 9]. It is a challenging manoeuvre that requires a series of careful actions to include maintaining optimal speed while ensuring accident avoidance and passenger comfort [10]. The author of [11] proposed fuzzy longitudinal control for manoeuvring AVs with safety. Furthermore, in [12, 13], a fuzzy logic controller is designed that takes an input from a camera and GPS to detect speed and distance between two vehicles. A sliding mode controller is suggested and implemented in [14] to the control lateral motion of vehicles before and after manoeuvring to avoid collisions. Relative position of vehicles and driving behaviour analysis based on fuzzy inference systems combined with a pre-established decision system based on the Q-system are suggested in [15]. The problem with the above discussed techniques is that they only work better for a limited scenario and in specific road conditions. Model predictive control (MPC) is adopted in [16] for manoeuvring to systematically handle stability limits, states, and entry restrictions. The behaviour of the controller changes with the variation in the scenario so the nonlinear behaviour of the MPC limits its implementation. In [17, 18], the author uses MPC with the sigmoid function for manoeuvring to avoid collisions. The author in [19] also proposed an MPC based on the probability of conflicts and the presence of unavoidable obstacles through the involved coordinates. A very important factor that should be considered during manoeuvring is timely communication between the vehicles. Therefore, in [20] CARRS-Q (the

advanced driving simulator-2011) is utilized for communication purposes. It also aided in connecting environmental conditions to the vehicles. In [21], the author analysed the driving behaviour along with environmental effects during the discretionary lane changing (DLC) manoeuvre. While in [22], a manoeuvring technique based on only communication between the vehicles is proposed and is implemented using a fuzzy control system, but it caters to only limited scenarios. In [23], the author used RGB-D data captured using Kinect devices in simulated traffic scenes. In this method, objects are tracked and detected using robust 3D tracking algorithms. The behaviour of the detected vehicle is analysed for different scenarios during manoeuvring. This technique is practiced in two-lanes only. An efficient and intelligent system based on a vision-based algorithm is proposed in [24]. A camera is required for each vehicle, which makes this system less feasible. A heuristic algorithm is proposed in [25] for speed planning on a two-lane road considering the approach time, vehicle's width, lane width, length ahead, and environment conditions. The quadratic optimization model is also implemented by the same author. A linearly parameter-varying approach is suggested in [26], but it requires reference manoeuvring parameters, which limits its implementation feasibility. A hierarchical scheme is also proposed in [26], which assists the driver. It uses the speed and acceleration signals of the surrounding vehicles and uses them for clustering to achieve the maximum probability density function. In [27], the author proposed manoeuvring technique based on variation in speed. This technique is simulated on Prescan and in MATLAB. A rough set theory-based approach is proposed in [28], but it works better only for two vehicles and two-lanes only.

An incremental search algorithm is proposed in [29] to ensure the shortest merging path. The author in [30] suggests a sampling-based trajectory planning technique for the same purpose. Manoeuvring trajectories are generated using the potential field method by compromising emergency situations in [31, 32]. This proposed technique is very much complex and requires a lot of computational power. A deep learning model is implemented in [33] for safe and secure manoeuvring, but a huge dataset is required for testing and training of the proposed model. Trajectory optimization for a safe path is proposed in [34]. It reduces intrusion onto the adjacent lane. This proposed technique is not implemented further due to its slow processing nature. 3010 vehicles are analysed in China, and it has been recorded that manual vehicles are comparatively fast in overtaking than electric vehicles [35]. Manoeuvring trajectory is divided into multiple short time trajectories to manipulate a safe path by [36]. But this technique becomes complex for the three-lane road. Different techniques are implemented for safe and quick manoeuvres, while very few discuss different possible scenarios. In [37] AVs manoeuvring is taken as an optimization problem, and Pontryagin's minimum principle is used to reduce the fuel consumption by 18% during the manoeuvring period. However, the constraints of the said scenario do not fit every vehicle and high-density traffic.

The contribution of this research work is to propose a navigational approach using rendezvous guidance (RG) for

the merging and leaving of the highway/convey of a vehicle coming down from the ramp to the highway. A modified form of the RG method is also implemented on the same problem. The operations are complex because of the need to pay attention to vehicles in two different lanes. Another additional scenario of leaving from center lane and joining sideways through the ramp is also solved using the same technique. Comparative analysis is also performed among the RG technique and its modified form. The proposed technique is also validated through experiments.

The major contributions of our research work are as follows:

- (1) Devising a merging and leaving the highway manoeuvring technique for vehicles coming through a ramp and a joining busy highway using the RG technique and its modified form
- (2) Devising a merging scenario in the presence of blocking vehicles
- (3) Devising a scenario for leaving from center lane and joining sideways through the ramp
- (4) Comparative analysis is performed to validate the effectiveness of the proposed approach

The proposed technique (modified RG) yields less lane change and merging time in comparison with the RG technique. In addition, the decisions in these complex merging scenarios have always been made considering the safety and comfort of the chasing vehicle user.

3. Mathematical Modelling and Problem Formulation

As discussed earlier, the main objective of this research is to propose and implement the merging and leaving the highway technique, which ensures safety and comfort to the vehicle and driver. A comfortable ride is reliant upon the values of lateral and angular acceleration, which should not exceed 1.25 m/s^2 and 5 m/s^2 , respectively. At least a time interval of 2 seconds is required for a safe distance between vehicles to realize collision-free braking operation [38–40]. Numerical values of braking distance and ride comfort are integrated as constraints in a proposed mathematical model. The proposed model will ensure safe and time-efficient lane changing.

The understanding of some terminologies is required to grasp the details of a mathematical model. The chasing vehicle is labelled as C , the leading vehicle is labelled as L , and the blocking vehicle (if any) in driving lane is labelled as OB . To ensure successful merging, the velocity of C must be greater than L . The velocities of C and L are given by v_c and v_l . In case, if OB is present in driving lane then C must adjust its velocity. Once OB clears driving lane, then C can proceed ahead for performing merging to highway. In this study, the time-efficient operations are performed using the rendezvous guidance (RG) technique and it is elaborated under Section 3.1. Although, with the proposed methodology, vehicle can even accelerate more, the cutoff is the speed limit on the road which is taken as 100 Km/hr , the highway limit. However, if the speed limit is increased, time may be further reduced.

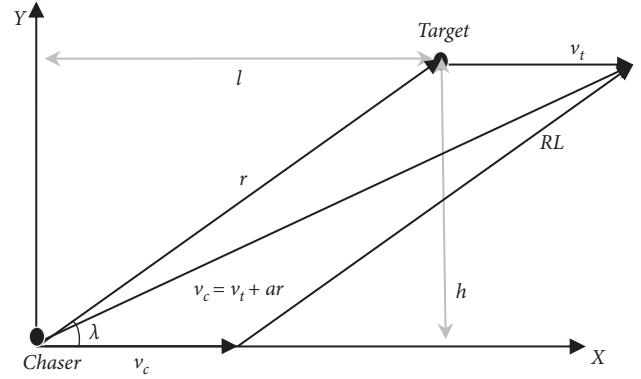


FIGURE 1: Construction of the rendezvous line (RL).

3.1. Rendezvous Guidance Technique. The RG technique was initially designed for rendezvous missions having asteroids and space stations [19, 20], but its results are also promising in the domain of nonmanoeuvring target interception. The use of RG for AVs is restricted by the limitation i.e., RG is designed to match velocity with the target, but in the case of AVs, there is no target; hence, a virtual/shadow target is needed, which will guide C through all phases of manoeuvring with safety and comfort. The locations of the shadow target will be determined as per the location of C and OB . The RG technique mentioned in [41–45] laid stress on gathering relevant information of C , L , and OB which is used for generating acceleration command for C . The acceleration command is determined via velocity matching of C with shadow targets considering user comfort and chasing vehicle dynamics.

3.2. Rendezvous Guidance Law-Based Trajectory. Consider a two-dimensional environment involving C and a shadow target having velocities of v_c and v_t , respectively. The imaginary line that connects C and shadow target is referred to as line-of-sight (LOS). The angle between LOS and x -axis is given in (1) which is also displayed in Figure 1. h is the distance between C and shadow target in a lateral direction while l is the distance between the two in an axial direction. The length of LOS is given as “ r ” and parallel navigation law states that direction LOS should be constant with respect to the nonrotating frame as C approaches the shadow target. Equations (2) and (3) represent the parallel navigation law mathematically.

$$\lambda = \tan^{-1} \frac{h}{l}, \quad (1)$$

$$r \times \dot{r} = 0, \quad (2)$$

$$r \cdot \dot{r} < 0. \quad (3)$$

The combination of (2) and (3) ensures that r and \dot{r} remains collinear and C shall not recede from the target. If we solve (2) and (3) in a parametric form, then the resulting expression would be (4). a is a positive real number in (4). The instantaneous velocity can be written in terms of the

difference between the velocities of shadow target and C as in (5). The substitution of (4) in (5) will yield mathematical expression (6).

$$\dot{r} = -ar, \quad (4)$$

$$\dot{r} = v_t - v_c, \quad (5)$$

$$v_c = v_t + ar. \quad (6)$$

The time-efficient chaser velocity command is obtained by substitution of r in (6) which results in a locus of vector v_c that lies on a semiline parameterized by a . This semiline is known as the rendezvous line also given in Figure 1. The endpoints of the vector v_c and v_t in Figure 1 demonstrate the positions of C and the shadow target after a unit time period, respectively. If C consistently follows the velocity command on RL, then the direction of LOS will always be constant, which ensures positional matching of C and the shadow target.

The next challenge is determining the value of α for realization of velocity matching. An early attempt at velocity matching may unnecessarily increase interception time so an efficient approach is to first determine the maximum allowable closing velocity without violating the velocity matching condition.

We assume that from the current instance until the realization of interception within a certain tolerance, C is only instructed by velocity commands that entirely lie on RL. This enables us to tackle the interception problems that are only focused in the LOS direction. We assume the acceleration of C in a particular direction to be given as A . The simultaneous reduction in velocity and position difference within LOS direction can be expressed as (7). The maximum magnitude of permissible closing velocity is indicated by r_{\max}^{rend} and t_r is time remaining from the current instant to the intercept. After solving (7), the expression of the maximum permissible velocity is given in (8). The maximum closing velocity as per the frequency of the velocity command for fast asymptotic interception is given in (9). Finally, the value of the permissible closing velocity component for velocity command is given by solving (8) and (9) which yields an expression (10).

$$\begin{cases} r_{\max}^{\text{rend}} - At_r = 0, \\ r - r_{\max}^{\text{rend}} t_r + \frac{1}{2} At_r^2 = 0, \end{cases} \quad (7)$$

$$r_{\max}^{\text{rend}} = \sqrt{2rA}, \quad (8)$$

$$r_{\max}^{\text{cr}} = \frac{r}{n \cdot \Delta t}, \quad (9)$$

$$v_{\max}^{\text{rel}} = \min \langle r_{\max}^{\text{rend}}, r_{\max}^{\text{cr}} \rangle. \quad (10)$$

The extreme points of velocity command vectors on RL having smaller closing velocity component in comparison with v_{\max}^{rel} making a line segment from $v_c = v_t$ to $v_c = v_{c, \max}$ ($= v_t + v_{\max}^{\text{rel}} (r/\|r\|)$) are known as the rendezvous set (RS), which is also indicated by a red line in Figure 2.

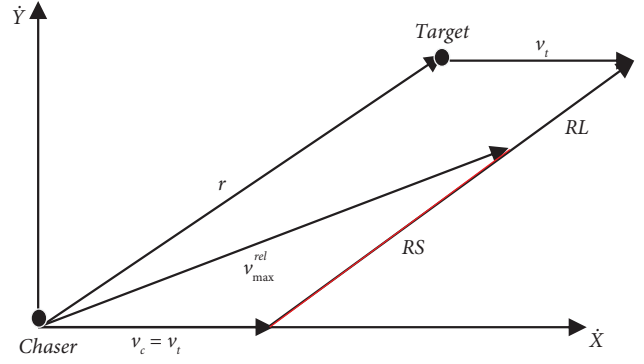


FIGURE 2: Construction of rendezvous set (RS).

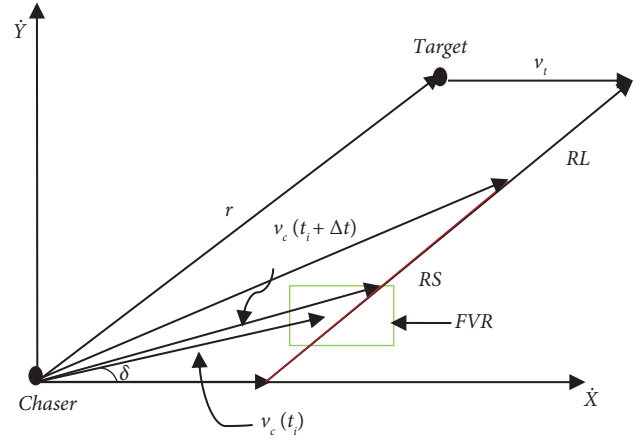


FIGURE 3: Construction of rendezvous set with feasible velocity region.

Sometimes velocity v_{\max}^{rel} cannot be achieved by C within Δt considering driver comfort and safety so a feasible region for range of velocities needs to be determined; see Figure 3. This region is determined by adding restrictions on the value of lateral acceleration of C. The maximum value for lateral acceleration of C can be determined by

$$a_{Y \max} = \frac{v_p^2}{Kh} 2 \sin^2 \vartheta \left(1 + \frac{\cos \vartheta}{\sqrt{K^2 - \sin^2 \vartheta}} \right), \quad (11)$$

where $a_{Y \max}$ is maximum lateral acceleration, $K = v_p/v_s$, h is the width of the lane, and ϑ is the maximum turning angle of chaser vehicle.

3.3. Modified Rendezvous Guidance Algorithm. The RG algorithm limits manoeuvrability due to unpredictability; however, movements on highways are predictable, and so it is possible to increase the velocity of C to decrease merging time while remaining within comfort and lateral acceleration constraints. This predictability offers us the opportunity to introduce another line, the velocity line (VL), which originates from the initial point of RL having an angle of ϑ with x -axis indicated as the purple line in Figure 4. Utilization of VL instead of RL ensures enhanced efficiency in merging and lane changing. If C follows VL instead of RL, the efficiency increases.

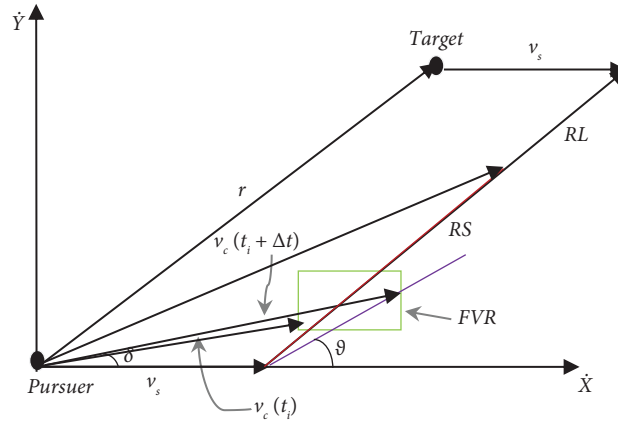


FIGURE 4: Construction of the velocity line.

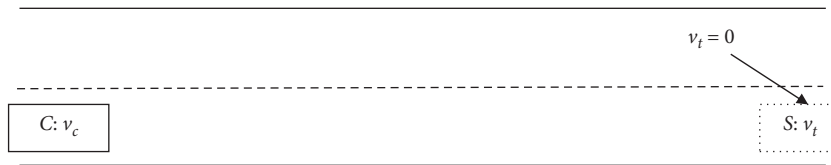


FIGURE 5: Stage 1.

4. Simulations Results and Comparison

The simulations of the proposed algorithm are conducted on a scenario of C joining the highway from the ramp. It is assumed that prior knowledge of all the vehicles in the workspace, including their size, location, and orientation, has been acquired in the real time through sensors installed on the autonomous vehicle. This information is used to estimate vehicles' trajectories and predict their future locations. Also, the simulation results show just the trajectory as a point mass; however, during simulations, the length and width of the vehicle is taken as 15 feet and 6 feet, respectively, and the width of the lane is taken as 10 feet. The distances given are from the back of the leading vehicle to the front of the chasing vehicle. We consider the velocity of C to be v_c on the ramp and the speed limit while joining the highway is defined as v_{Max} . The joining of highway is conducted in two different stages. The first stage involves C moving straight on a ramp and waits for the creation of a gap between vehicles on the highway. Stage 2 will come into effect once the gap is created between highway vehicles and C can safely change its lane from ramp to highway. As C enters a ramp, a static shadow target is formed at the end of ramp having $v_t = 0$ which marks the end of stage 1. Once the gap between highway vehicles is created, stage 2 begins with the formation of a static shadow target "S" being 3 s ahead of C having a velocity of v_{Avg} (the arithmetic average of v_c at a particular instant and v_{Max}) which is updated after very instance A . Additionally, when C leaves the center lane, it searches for gap in right or left driving lane, this is the manoeuvring stage 1, once AV finds the gap, it changes lanes and after 2 seconds of distance AV joins sideways through the ramp. The details of stage 1 and stage 2 are given in Figures 5 and 6. The simulations are performed in a visual basic environment.

4.1. Joining a Highway from Ramp without Obstacle Vehicle.

If there is no other vehicle present on the highway, which restricts C from joining the highway, then, as soon as C is on the ramp and is parallel to the highway, stage 2 starts, and C joins the highway by receiving the velocity and direction commands from the modified RG method. In this scenario, i.e., the maximum velocity C can achieve is the speed limit for that highway.

For this scenario, the velocity of C once it joins the ramp and is parallel to the highway is assumed to be 20 m/s and the speed limit for the highway, is defined as 30 m/s. At the start of stage 2, the average velocity, = 25 m/s. S is created 3 s before the current C 's location. C gets the velocity and direction commands from the modified RG method to rendezvous with S . The simulation plots for path and velocity of C for this case are given in Figure 7.

4.2. Joining a Highway from Ramp with Obstacle Vehicle.

If an obstacle vehicle is present on the highway, it makes it unsafe for C to join the highway due to less gap between C and O_p , then C must wait for O_p to move ahead until the distance between them increases by 3 s. In this scenario, C remains in stage 1 until a gap of 3 s is created. While in stage 1, S is created at the end of the ramp with a velocity of 0. Hence, C starts decelerating to match the velocity and location of S in Phase 1. However, as soon as the gap between the vehicles is more than 3 s, stage 2 starts, and C starts the lane changing manoeuvre. In contrast to the first scenario, the maximum velocity would be $v_{Max} = \min \langle v_{Limit}, v_{op} \rangle$.

For this scenario, the velocity of C , once it joins the ramp and is parallel to the highway is assumed to be 20 m/s, the speed limit for the highway v_{Limit} , is defined as 30 m/s, and the

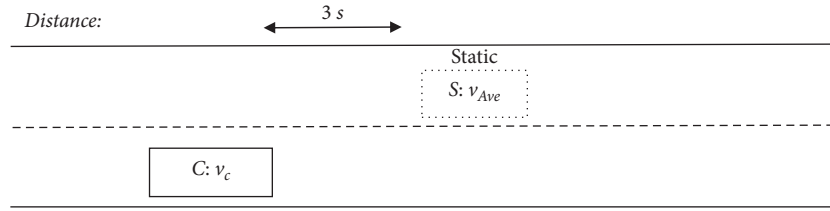


FIGURE 6: Stage 2.

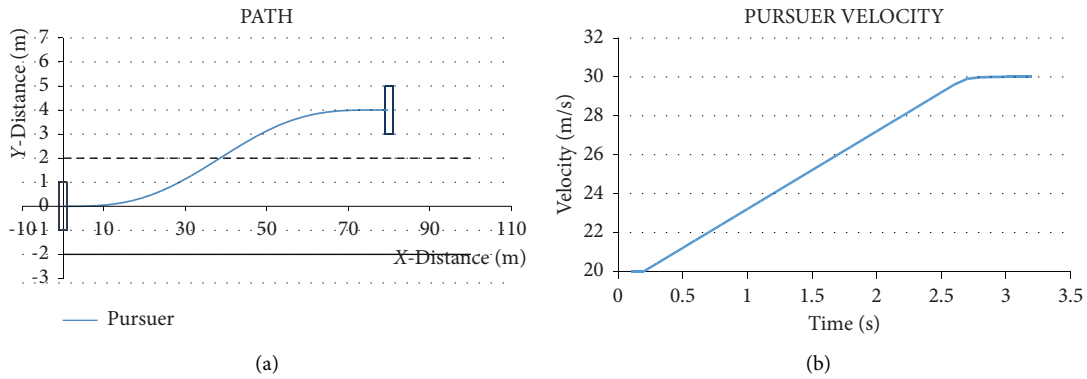


FIGURE 7: Joining highway without obstacle vehicle (plots for path and velocity of C).

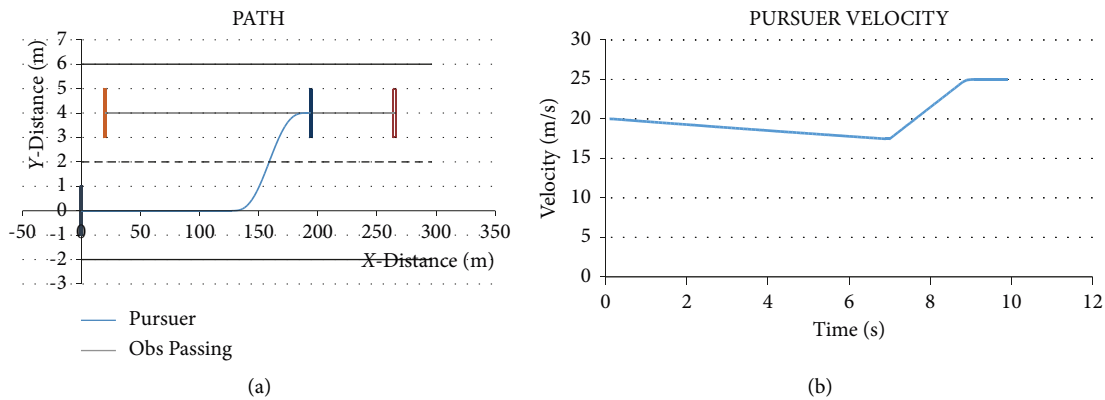


FIGURE 8: Joining highway with obstacle vehicle (plots for path and velocity of C).

obstacle vehicle's velocity on the highway is taken as 25 m/s. In this case, $v_{op} < v_{Limit}$, $v_{Max} = v_{op}$. The simulation plots for path and velocity of C for this scenario are given in Figure 8.

4.3. Joining a Sideway from Highway through Ramp with Obstacle Vehicle. In this scenario, C is initially on the center lane of the highway and wants to join the ramp, which is parallel to the highway; its initial velocity is assumed to be 20 m/s and speed limit v_{Limit} of the highway is taken as 30 m/s. C will change lanes first by finding the gap in the driving lane. However, C must wait in the center lane until the distance gets 3 s in the driving lane. Once it C changes lanes, then next stage is joining sideways through the ramp, which is simple. In this scenario, the speed limit changes, as the minimum speed between the first lane vehicle OB which is v_{OB} , and v_{Limit} is picked up for maximum permissible velocity of C. It is

assumed that OB is moving at 25 m/s; thus, $v_{OB} < v_{Limit}$ and $v_{Max} = v_{OB}$. Therefore, C can have the maximum velocity of 25 m/s for safe lane changing.

4.4. Comparison of Conventional and Modified RG Method. The simulations are performed for all three cases using the conventional RG method and its modified form. Two different parameters are considered for comparisons which are total time taken and distance covered for lane changing from ramp to passing lane on a highway. The results of both methods are given in Table 1. The time taken for lane changes is 13.4% less for the modified RG method in comparison with the conventional RG method. Similarly, the distance covered while lane changing is 15.4% less in the modified method when compared to the conventional RG method.

TABLE 1: Comparisons of modified and conventional RG algorithm simulation results.

Parameters	Modified RG methods	Conventional RG methods
Total time (s)	8.75	10.1
Distance travelled (m)	190	225

5. Experimental Setup and Results

5.1. Experimental Setup. The experiments were conducted with the intention of performing a comparative analysis of the modified and conventional RG methods. These experiments are performed on differential drive robots. Experimental results exhibit a similar trend as simulation results.

The image of the workspace is captured and processed to collect relevant information about all objects in the workspace. The image acquisition and processing module of software is used for collecting workspace object information. The extracted information is used for the calculation of the command that needs to be sent to chasing robot. Software used in experimental trials comprises of three main modules which are image acquisition and processing, communication modules, and trajectory planning. The first stage involves capturing workspace images through a CCD camera. The second stage extracts positional information through a vision algorithm. Finally, the third stage sends the extracted information to the trajectory planner for determining the acceleration command of the chasing robot.

Although three levels of autonomy exist in AVs (fully autonomous, semiautonomous, and driver-assisted), but for hardware validation, we have not considered the role of the driver because proposed technique is experimentally implemented using robots. We have considered merging and leaving the highway only, while AV has many other operations too.

The detailed process flow diagram is shown in Figure 9. Physical layout of the experimental setup is shown in Figure 10. The workspace of searching lane markers is shown in Figure 11 and robotic vehicles along with colored markers are shown in Figure 12.

5.1.1. Vision System

(1) *Hardware.* The vision system consists of a CCD camera that comes along with a wide-angle lens and frame capturer Matrox Meteor-II. The camera used in the experiment has a color output that is standard composite and has 640×480 pixels' resolution. CCD cameras have 30 frames per second (fps) refresh rate. The field of view (FOV) is $3200 \text{ mm} \times 2400 \text{ mm}$. The calibration model for a camera is used to convert a coordinate image to a world transformation. The off-line technique used in [46], which is non-coplanar is used in our overhead camera.

(2) *Software.* The color coding of the obstacle vehicle and pursuer vehicle was done for the purpose of identification. The raw images incorporate the data of three different colors with various intensities that correspond to three different channels. These three colors are red (R), green (G), and blue

(B). 8 bits of information can be added to a single channel. Therefore, a total of 24 bits of information can be added to one pixel, which corresponds to 16 million color possibilities. However, only three colors are utilized by identification markers. Thus, 24 bits based information must be categorized within these three colors or the fourth category could be noncolor through the thresholding process.

The work floor is thoroughly searched for identification of vehicle markers. The sampling is performed as per markers identified to have a minimal search period. The smallest maker's dimensions are utilized for defining the minimum sampling rate. If, a pixel that is sampled contains color from a predefined set, then, a search frame is embedded onto the pixel. The search frame's size is reliant upon the color of interest, but at least it has twice the marker's diameter. The particular size of the search frame guarantees that irrespective of orientation, the marker shall remain within the frame. The examination of each pixel that lies within the search frame is conducted. If a particular color pixel's strength surpasses the threshold value, then that color's marker is considered to be situated in the vicinity of the search frame. The particular operation is performed for the entire floor of a workspace to identify all color markers. Once the makers are identified, the process of object identification begins. The color-coded markers are utilized for identification of P , O_D , and O_P . The vision program begins to search for colored circle markers. The difference in color in the circular marker pattern helps in the identification of vehicles among P , O_D , and O_P . If P gets identified, then, it is represented by blue color. O_D gets identified with a red circle and O_P gets recognized with a yellow circle.

5.1.2. Robotic Vehicles. Three similar robotic vehicles are used for the experiment; all the robots are MIABOT pro robots. These robots possess a differential driving system and are autonomous, which alleviates their compactness and implementation. The unloaded motor can achieve a maximum speed between 6000–8000 rpm. The wheels of robots are driven through 8 : 1 gearing via motor shafts. The quadrature encoders are added within the motors which provide 512 positional pulses against each rotation. As the diameter of the wheels is 52 mm so a single pulse of the encoder corresponds to 0.4 mm of movement. The orientation and position of a vehicle are then determined by marking the top plates with a colored pattern. This particular information is then provided to a vision system. The communication system comprises of a Bluetooth module which is responsible for a frequency hopping communication protocol at a frequency of 2.4 GHz. The incorporation of Bluetooth card in robots enables the host PC to interact with the vehicle. The communication between

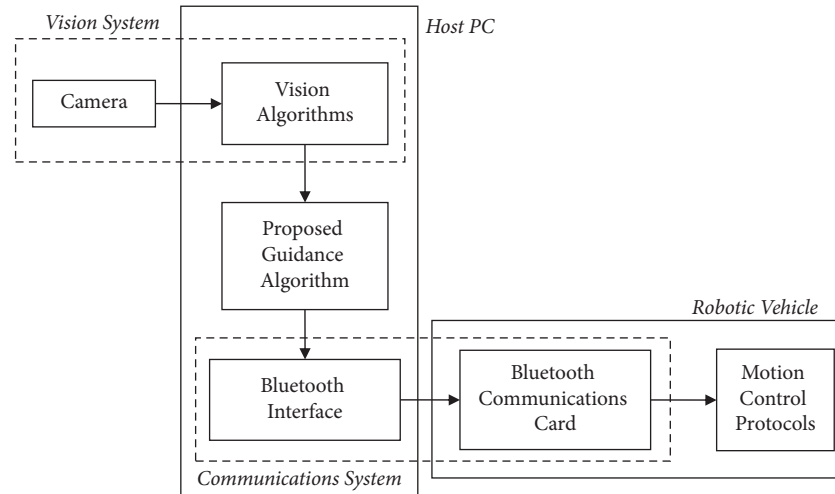


FIGURE 9: Experimental setup: software process flow diagram.

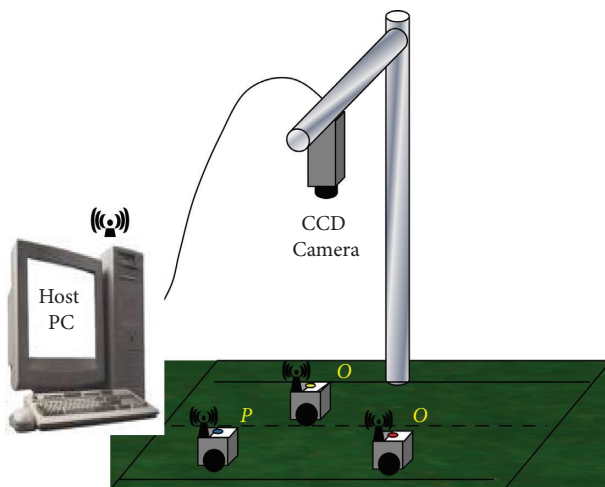


FIGURE 10: Experimental setup: physical layout.

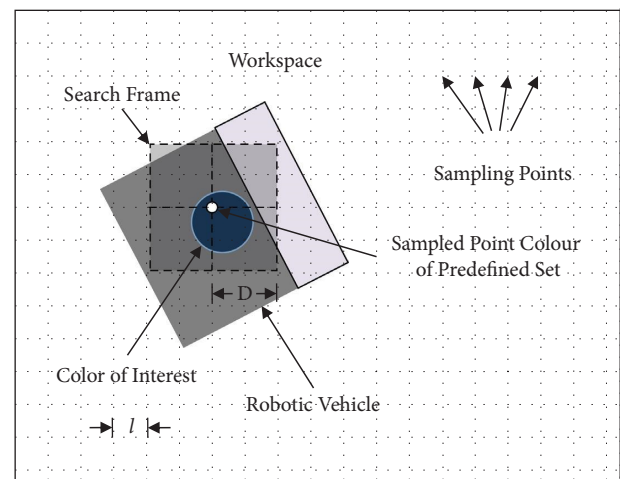


FIGURE 11: Searching for color marker.

them occurs via the conversion of Bluetooth link to logic-level serial signals that are connected to the main board processor.

5.2. Experiment Results. For the experiments, the initial velocity of C is taken to be 10 mm/s. Two cases of ramp merging are evaluated. The first case of ramp is like case 1 because of nonpresence of obstacle, while in the second case of ramp merging consists of obstacle vehicle. Decision taking by the chaser vehicle is comparatively easy in the first case of ramp merging than the second. Since the second case faces an obstacle vehicle having nonuniform velocity. While in the additional scenario, where C wants to join sideways from the center lane of the highway through a ramp, the first stage is the same as reverse overtaking manoeuvring in the presence of an obstacle as presented in [3].

Experiments were conducted using the proposed modified RG technique and original RG technique. In the case, when an obstacle vehicle is present in the merging lane,

C takes the velocity of the obstacle into the account. The decision in this scenario is dependent upon the distance and speed of the obstacle vehicles. Since an obstacle vehicle moves with nonuniform velocity so C merges with non-uniform speed.

Critically analyzing experimental results, the following results are concluded:

- (1) Adopting modified RG techniques, vehicles travel less distance. In millimeter scale, a vehicle relocates itself after travelling 90 mm.
- (2) When it adopts simple RG techniques, it travels 96 mm distance to relocate itself after merging.
- (3) Modified RG results in less time when compared to simple RG. In the merging case, modified RG arrives 1.5 seconds earlier than simple RG.

Simulation results are approximately justified with 96% accuracy. The experimental plots of both scenarios for path and velocity of P are given in Figures 13(a)–13(d).

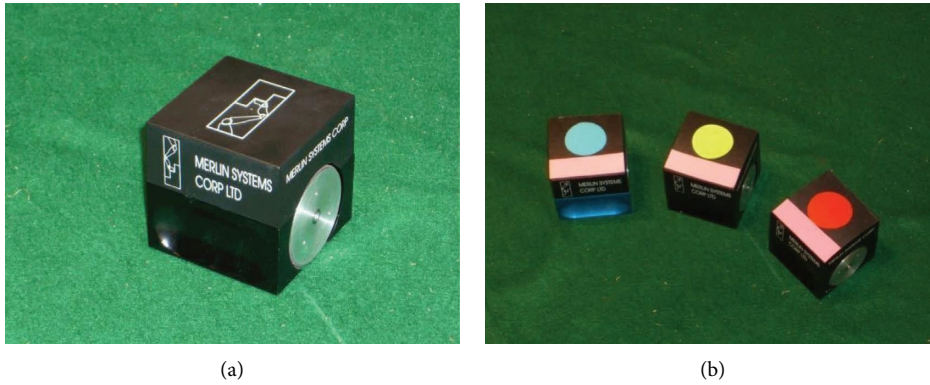


FIGURE 12: (a) Robotic vehicle and (b) vehicles with markers.

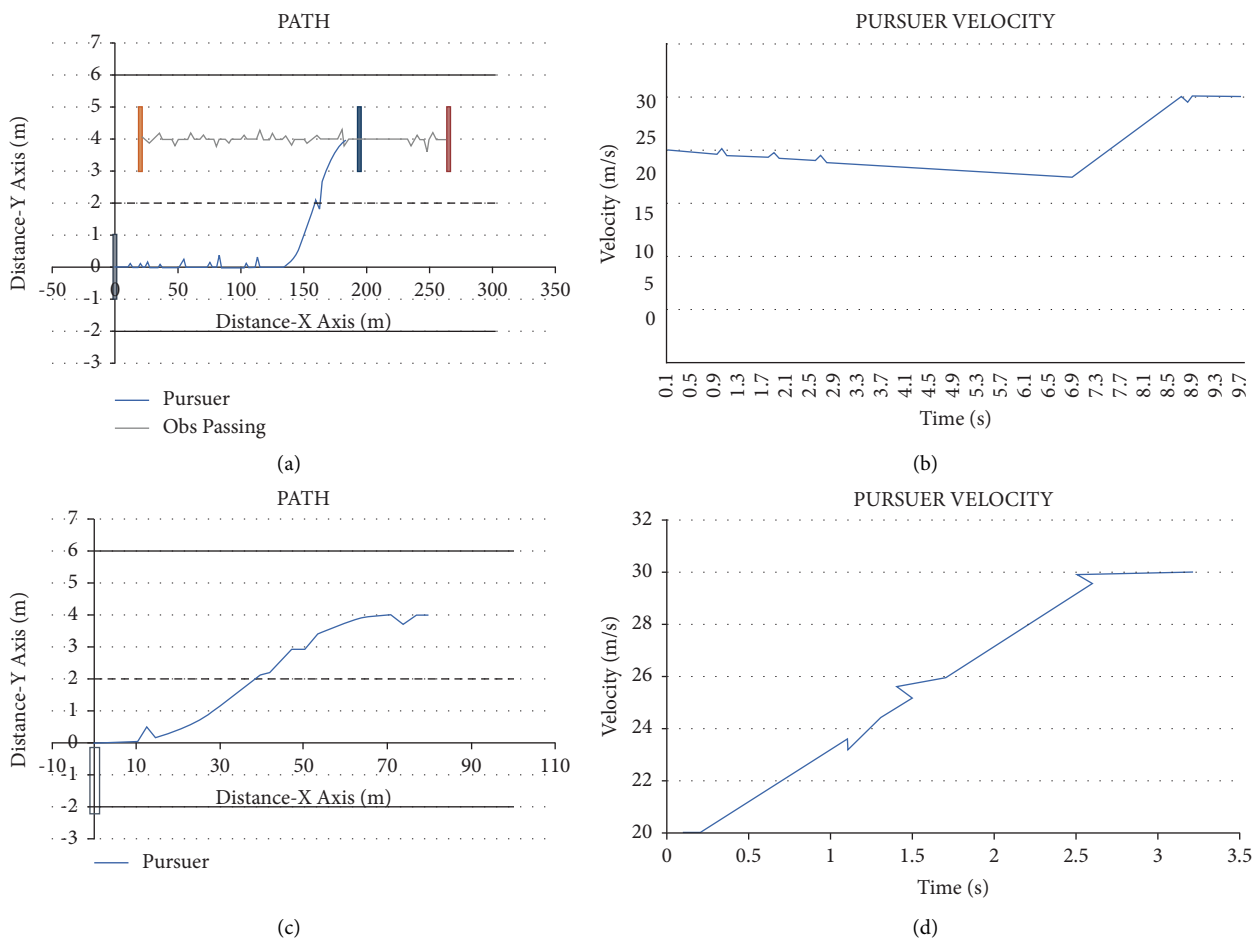


FIGURE 13: (a) Path of P . (b) Velocity plot of P . (c) Path of P . (d) Velocity plot of P .

6. Conclusions

This research work presents a time-efficient guidance-based algorithm for navigating the AVs during merging and leaving the highway through a circular ramp. Two scenarios are presented (merging onto a highway and leaving a highway). In both cases, further permutation includes the presence or absence of any other vehicle in the workspace. The simulation results

demonstrate that, in the case of the presence of an obstacle vehicle on the highway, the presented approach demonstrates adaptability in ensuring that an optimal gap of 3 s is ensured between the chasing and obstacle vehicles for smooth lane changing. In addition, the shadow target at the end of the ramp will enable the chasing vehicle to gradually lower its speed as it approaches the shadow target to avoid collision. Although the modified RG algorithm ensures user comfort and safety, but still future

work needs to be done upon lane changing considering multiple vehicles entering from ramp to the highway. Also, since a lot of electronics and IC's are utilized in the hardware of autonomous vehicle and imperfections in these due to the nonlinearity of the model could affect the efficacy of the system. Hence, the effects of these need to be studied as a new research subject based on imperfect systems [47].

Abbreviations

RG:	Rendezvous guidance
MPC:	Model predictive control
S:	Shadow target
L:	Leading vehicle
C:	Chasing vehicle
OB:	Blocking vehicle
RL:	Rendezvous line
VL:	Velocity line
v_c :	Velocity of C
v_l :	Velocity of L
v_t :	Velocity of shadow target
LOS:	Line-of-sight
λ :	LOS angle with fixed reference (X-axis)
h :	Distance between chasing vehicle and shadow target in a lateral direction
r :	Length of LOS
\dot{r} :	Relative velocity
t_r :	Remaining time-to-intercept from current instant
\dot{r}_{\max}^{cr} :	Maximum closing velocity for fast asymptotic interception
v_{\max}^{rel} :	Final value of allowable closing velocity component
RS:	Rendezvous set
Δt :	Time interval
$a_{Y \max}$:	Maximum lateral acceleration
h :	Width of lane
ϑ :	Maximum turning angle of chasing vehicle
δ :	Current heading angle of chasing vehicle
FVR:	Feasible velocity region
v_{RG} :	Desired velocity of chasing vehicle in upcoming instant by modified RG method
a_{RG} :	Desired acceleration of chasing vehicle in upcoming instant by modified RG method
NFVR:	New feasible velocity region
l :	Distance between chasing vehicle and shadow target in an axial direction
A :	Acceleration of chaser vehicle
$\dot{r}_{\max}^{\text{rend}}$:	Maximum magnitude of closing velocity.

Data Availability

The data used to support the findings of this study are available from the corresponding author upon request.

Conflicts of Interest

The authors declare that they have no conflicts of interest.

References

- [1] H. Prakken, "On the problem of making autonomous vehicles conform to traffic law," *Artificial Intelligence and Law*, vol. 25, no. 3, pp. 341–363, 2017.
- [2] B. van Arem, C. J. G. van Driel, and R. Visser, "The impact of cooperative adaptive cruise control on traffic-flow characteristics," *IEEE Transactions on Intelligent Transportation Systems*, vol. 7, no. 4, pp. 429–436, 2006.
- [3] U. Ghumman, H. Jabbar, M. I. Tiwana, I. U. Khalil, and F. Kunwar, "A novel approach of overtaking maneuvering using modified RG method," *PLoS One*, vol. 17, no. 1, Article ID e0260455, 2021.
- [4] S. Pettigrew, Z. Talati, and R. Norman, "The health benefits of autonomous vehicles: public awareness and receptivity in Australia," *Australian & New Zealand Journal of Public Health*, vol. 42, no. 5, pp. 480–483, 2018.
- [5] W. Huang, K. Wang, Y. Lv, and F. Zhu, "Autonomous vehicles testing methods review," in *Proceedings of the 2016 IEEE 19th International Conference on Intelligent Transportation Systems (ITSC)*, pp. 163–168, Rio de Janeiro, Brazil, 2016.
- [6] J. Ortega, J. Hamadneh, D. Esztergár-Kiss, and J. Tóth, "Simulation of the daily activity plans of travelers using the park-and-ride system and autonomous vehicles: work and shopping trip purposes," *Applied Sciences*, vol. 10, no. 8, p. 2912, 2020.
- [7] J. T., T. P. Ortega, J. Tóth, T. Peter, and S. Moslem, "An integrated model of park-and-ride facilities for sustainable urban mobility," *Sustainability*, vol. 12, no. 11, p. 4631, 2020.
- [8] L. Barr and W. Najm, "Crash problem characteristics for the intelligent vehicle initiative", presented at the transportation research board 80th annual meeting, 2001," 2021, <https://trid.trb.org/view/675725>.
- [9] K. Anindyaguna, N. C. Basjaruddin, and D. Saefudin, "Overtaking assistant system (OAS) with fuzzy logic method using camera sensor," in *Proceedings of the 2016 2nd International Conference of Industrial, Mechanical, Electrical, and Chemical Engineering (ICIMECE)*, pp. 89–94, Yogyakarta, Indonesia, 2016.
- [10] K. Osman, J. Ghommam, and M. Saad, "Guidance based lane-changing control in high-speed vehicle for the overtaking maneuver," *Journal of Intelligent and Robotic Systems*, vol. 98, no. 3-4, pp. 643–665, 2020.
- [11] J. Pérez, V. Milanés, E. Onieva, J. Godoy, and J. Alonso, "Longitudinal fuzzy control for autonomous overtaking," in *Proceedings of the 2011 IEEE International Conference on Mechatronics*, pp. 188–193, Beijing, China, Apr. 2011.
- [12] *Lane-Change Fuzzy Control in Autonomous Vehicles for the Overtaking Maneuver*, IEEE, New York, Ny, USA, 2021.
- [13] J. Ortega, J. Tóth, and T. Péter, "Mapping the catchment area of park and ride facilities within urban environments," *ISPRS International Journal of Geo-Information*, vol. 9, p. 501, 2020.
- [14] M. Durali, G. A. Javid, and A. Kasaiezadeh, "Collision avoidance maneuver for an autonomous vehicle," in *Proceedings of the 9th IEEE International Workshop on Advanced Motion Control, 2006*, pp. 249–254, Istanbul, Turkey, Mar. 2006.
- [15] M. Zhang, T. Zhang, and Q. Zhang, "An autonomous overtaking maneuver based on relative position information," in *Proceedings of the 2018 IEEE 88th Vehicular Technology Conference (VTC-Fall)*, pp. 1–6, Chicago, IL, USA, Aug. 2018.

- [16] A. Gray, Y. Gao, T. Lin, J. K. Hedrick, H. E. Tseng, and F. Borrelli, "Predictive control for agile semi-autonomous ground vehicles using motion primitives," in *Proceedings of the 2012 American Control Conference (ACC)*, pp. 4239–4244, Quebec, Canada, Jun. 2012.
- [17] J. Nilsson, M. Ali, P. Falcone, and J. Sjöberg, "Predictive manoeuvre generation for automated driving," in *Proceedings of the 16th International IEEE Conference on Intelligent Transportation Systems (ITSC 2013)*, pp. 418–423, Hague, The Netherlands, Oct. 2013.
- [18] X. Huang, W. Zhang, and P. Li, "A path planning method for vehicle overtaking maneuver using sigmoid functions," *IFAC-Papers Online*, vol. 52, no. 8, pp. 422–427, 2019.
- [19] F. Wang, M. Yang, and R. Yang, "Conflict-probability-estimation-based overtaking for intelligent vehicles," *IEEE Transactions on Intelligent Transportation Systems*, vol. 10, no. 2, pp. 366–370, 2009.
- [20] Y. Ali, A. Sharma, M. M. Haque, Z. Zheng, and M. Saifuzzaman, "The impact of the connected environment on driving behavior and safety: a driving simulator study," *Accident Analysis & Prevention*, vol. 144, Article ID 105643, 2020.
- [21] Y. Ali, Z. Zheng, M. D. MazharulHaque, M. Yildirimoglu, and S. Washington, "Understanding the discretionary lane-changing behaviour in the connected environment," *Accident Analysis & Prevention*, vol. 137, Article ID 105463, 2020.
- [22] C. Mo, Y. Li, and L. Zheng, "Simulation and analysis on overtaking safety assistance system based on vehicle-to-vehicle communication," *Automotive Innovation*, vol. 1, no. 2, pp. 158–166, 2018.
- [23] X. Yingjie, W. Chunhui, S. Xingmin, and Z. Luming, "Vehicles overtaking detection using RGB-D data-sciencedirect," *Signal Processing*, vol. 112, 2015.
- [24] V. Milanés, D. F. Llorca, J. Villagra et al., "Intelligent automatic overtaking system using vision for vehicle detection," *Expert Systems with Applications*, vol. 39, no. 3, pp. 3362–3373, 2012.
- [25] S. M. Easa and M. Diachuk, "Optimal speed plan for the overtaking of autonomous vehicles on two-lane highways," *Infrastructure*, vol. 5, p. 44, 2020.
- [26] B. Németh, P. Gáspár, and T. Hegedűs, *Journal of Advanced Transportation*, vol. 2018, Article ID 2195760, 11 pages, Optimal Control of Overtaking Maneuver for Intelligent Vehicles, 2018.
- [27] M. Yousef, A. Hosny, W. Gamil et al., "Dual-mode forward collision avoidance algorithm based on vehicle-to-vehicle (V2V) communication," in *Proceedings of the 2018 IEEE 61st International Midwest Symposium on Circuits and Systems (MWSCAS)*, pp. 739–742, East Lansing, MI, USA, Aug. 2018.
- [28] X. Chen, Y. Miao, M. Jin, and Q. Zhang, "Driving decision-making analysis of lane-changing for autonomous vehicle under complex urban environment," in *Proceedings of the 2017 29th Chinese Control and Decision Conference (CCDC)*, pp. 6878–6883, Yichang, China, May 2017.
- [29] L. Ma, J. Xue, K. Kawabata, J. Zhu, C. Ma, and N. Zheng, "A fast RRT algorithm for motion planning of autonomous road vehicles," in *Proceedings of the 17th International IEEE Conference on Intelligent Transportation Systems (ITSC)*, pp. 1033–1038, Indianapolis, IN, USA, Oct. 2014.
- [30] "Application of sampling-based motion planning algorithms in autonomous vehicle navigation, intechopen," 2021, <https://www.intechopen.com/chapters/51781>.
- [31] "Autonomous vehicle trajectory planning and control based on virtual di," 2021, <https://www.taylorfrancis.com/chapters/edit/10.1201/9781315265285-130/autonomous-vehicle-trajectory-planning-control-based-virtual-disturbance-compensation-via-simulation-feedback-control-systems-raksincharoensak-ehira-shimono-tagawa>.
- [32] C. Katrakazas, M. Quddus, W.-H. Chen, and L. Deka, "Real-time motion planning methods for autonomous on-road driving: state-of-the-art and future research directions-sciencedirect," *Transportation Research Part C: Emerging Technologies*, vol. 60, 2015.
- [33] M. Kaushik, V. Prasad, K. M. Krishna, and B. Ravindran, "Overtaking maneuvers in simulated highway driving using deep reinforcement learning," in *Proceedings of the 2018 IEEE Intelligent Vehicles Symposium (IV)*, pp. 1885–1890, Changshu, China, Jun. 2018.
- [34] J. Palatti, A. Aksjonov, G. Alcan, and V. Kyrki, "Planning for safe abortable overtaking maneuvers in autonomous driving," 2021, <https://arxiv.org/abs/2104.00077>.
- [35] Y. Liu, C. Fu, and W. Wang, "Modeling duration of overtaking between non-motorized vehicles: a nonparametric survival analysis based approach," *PLoS One*, vol. 16, no. 1, Article ID e0244883, 2021.
- [36] S. M. Zhang, H. Sun, and Y. Wang, "A trajectory planning algorithm for autonomous overtaking maneuvers," *Applied Mechanics and Materials*, vol. 347–350, pp. 3494–3499, 2013.
- [37] J. Zhao, V. L. Knoop, and M. Wang, "Two-dimensional vehicular movement modelling at intersections based on optimal control," *Transportation Research Part B: Methodological*, vol. 138, pp. 1–22, 2020.
- [38] M. R. Koopman and L. J. J. Kusters, "The development of a path planning strategy for obstacle avoidance and crash impact minimisation for an automatic guided vehicle," *Advanced Chassis and Transport Systems*, vol. 73, p. 77, 2003.
- [39] Z. Shiller and S. Sundar, "Emergency lane-change maneuvers of autonomous vehicles," *Journal of Dynamic Systems, Measurement, and Control*, vol. 120, no. 1, pp. 37–44, 1998.
- [40] M. Omae and T. Fujioka, "DGPS-based position measurement and steering control for automatic driving," in *Proceedings of the American Control Conference*, pp. 3685–3690, San Diego, California, 1999.
- [41] M. Mehrandezh, N. Sela, R. G. Fenton, and B. Benhabib, "Robotic interception of moving objects using an augmented ideal proportional navigation guidance technique," *IEEE Transactions on Systems, Man, and Cybernetics-Part A: Systems And Humans*, vol. 30, no. 3, pp. 238–250, 2000.
- [42] J. M. Borg, M. Mehrandezh, R. G. Fenton, and B. Benhabib, "Navigation-guidance-based robotic interception of moving objects in industrial settings," *Journal of Intelligent and Robotic Systems*, vol. 33, no. 1, pp. 1–23, 2002.
- [43] F. Agah, M. Mehrandezh, R. G. Fenton, and B. Benhabib, "Rendezvous-guidance based robotic interception," in *Proceedings of the IEEE International Conference on Intelligent Robots and Systems*, pp. 2998–3003, Las Vegas, NV, USA, Oct. 2003.
- [44] F. Kunwar, F. Wong, R. Ben Mrad, and B. Benhabib, "Rendezvous guidance for the autonomous interception of moving objects in cluttered environments," in *Proceedings of the IEEE International Conference of Robotics and Automation*, Barcelona, Spain, April 2005.
- [45] F. Kunwar and B. Benhabib, "Motion planning for autonomous rendezvous with vehicle convoys| proceedings of the IEEE ITSC," in *Proceedings of the 2006 IEEE Intelligent*

Transportation Systems Conference, Toronto, Canada, September, 2006.

- [46] D. Chai and A. Bouzerdoum, "A Bayesian approach to skin color classification in YCbCr color space," *TENCON Proceedings. Intelligent Systems and Technologies for the New Millennium (Cat. No. 00CH37119)*, vol. 2, pp. 421–424, 2000.
- [47] M. Bucolo, A. Buscarino, C. Famoso, L. Fortuna, and S. Gagliano, "Imperfections in integrated devices allow the emergence of unexpected strange attractors in electronic circuits," *IEEE Access*, vol. 9, pp. 29573–29583, 2021.